

**Transverse azimuthal dephasing of a vortex spin wave in a hot atomic gas**Shuai Shi, Dong-Sheng Ding,\* Wei Zhang, Zhi-Yuan Zhou, Ming-Xin Dong, Shi-Long Liu,  
Kai Wang, Bao-Sen Shi,† and Guang-Can Guo<sup>1,2</sup>*Key Laboratory of Quantum Information, University of Science and Technology of China, Hefei, Anhui 230026, China  
and Synergetic Innovation Center of Quantum Information & Quantum Physics, University of Science and Technology of China,  
Hefei, Anhui 230026, China*

(Received 12 August 2016; published 20 March 2017)

An optical field with orbital angular momentum (OAM) has many remarkable properties due to its unique azimuthal phase, showing many potential applications in high-capacity information processing such as terabit free-space data transmission, and high-precision measurement such as high sensitivity of angular resolution. The dephasing mechanisms of optical fields in an interface between light and matter play a vital role in OAM storage. In this work, we study the transverse azimuthal dephasing of an OAM spin wave in a hot atomic gas via OAM storage. We find that the transverse azimuthal phase difference between the control and probe beams is mapped onto the spin wave, and the atomic motion during the storage results in dephasing of the atomic spin wave with transverse azimuthal phase. The dephasing of the OAM spin wave is related to the OAM's topological charge and the beam waist. Our results are helpful for studying OAM light interaction with matter.

DOI: [10.1103/PhysRevA.95.033823](https://doi.org/10.1103/PhysRevA.95.033823)

Studying and controlling the quantum states of the collective excitations of atoms is conducive to the development of a quantum repeater, which is required for long-distance quantum communication [1,2]. Especially, coherent storage and manipulation of quantum superposition states is essentially important to ensure high-fidelity evolution. Recently, mechanisms responsible for the decoherence of atomic states attract many researchers in quantum optics and atomic physics fields [3,4], because the atomic system can be used as a reliable and long-lived storage unit for quantum communications [5].

A light pulse can be stored as a collective excitation and read out in atomic vapor [6,7]. The transverse amplitude and phase profile of the pulse can be preserved very well for a short-time storage [8], but the fidelity of a long-time storage will be seriously affected by the atomic motion during the storage [9]. There are two main kinds of dynamics that underlie the decoherence mechanisms in the atomic vapor: the collisions among atoms and with the internal wall of the vapor cell, and the random thermal motion of the atoms [3]. The decoherence caused by collisions can be improved effectively by coating the inner walls of a cell with an antirelaxation film, and adding buffer gas into the cell to keep the atoms in the illuminated region for a longer time [10,11]. Although the atomic motion can be utilized to freeze a light pulse in a coherently driven atomic medium and implement a controllable slow light beam splitter [12,13], it crucially affects the resolution and the coherence time of the stored optical images. The decoherence mechanisms induced by atomic motion attract a lot of attention; thus many techniques are used to overcome or reduce the decoherence. For example, the diffraction induced by atomic motion can be utilized to eliminate the paraxial diffraction at proper two-photon detuning [14], spin echo technology can be used to extend the atomic coherence time [15,16], storing the Fourier transform

of the image can overcome the adverse effects of diffusion [17], etc.

Light with OAM stored in hot atomic gas can maintain its phase singularity due to topological stability [18–20]. Storing light with OAM in hot atomic gas cannot only help to improve the capacity of quantum information processing [21,22], but also exploit the advantages of simplicity. However, various decoherence mechanisms significantly affect the fidelity of the collective excitations of atoms, such as random dephasing, the loss of atoms and atomic motion, etc. [4]. As a result, studying the dephasing of the OAM light interacting with hot atomic gas is crucially important. The phase front fluctuation induced by atomic random motion in the vector direction of the spin wave (SW) [23] directly affects the fidelity. While in the transverse radial direction, atoms carrying a phase from all directions destructively interfere at the dark center which is a phase singularity of the SW [20,24]. The dephasing in the transverse azimuthal direction resulting from phase front fluctuation is the topic of this work.

In this work, we introduce different OAM to the control beam to prepare the SW with a different topological charge. We show that a SW with a higher topological charge has a larger decoherence rate, and a theoretical analysis for the distinct decoherence mechanisms is given. Moreover, we experimentally observe an increase in the lifetime for OAM SW as the beam waist increases.

Optical fields near the  $D_1$  transition of  $^{85}\text{Rb}$  (795 nm) are used for electromagnetically induced transparency (EIT) and light storage. This light-storage technique has been proved experimentally [25,26]. The energy level scheme is presented in Fig. 1(c), which shows a  $\Lambda$  system and the control and probe transitions. An external cavity diode laser is stabilized to the  $F = 3 \rightarrow F' = 2$  transition. The laser is divided into a control beam and a probe beam which have orthogonal linear polarizations. The control beam passes through an acousto-optic modulator (AOM), so we can control both the frequency and the intensity of it. The control is red detuned about 300 MHz to the  $F = 3 \rightarrow F' = 2$  transition; the probe is blue detuned 3.035 GHz to the control after double

\*dds@ustc.edu.cn

†drshi@ustc.edu.cn

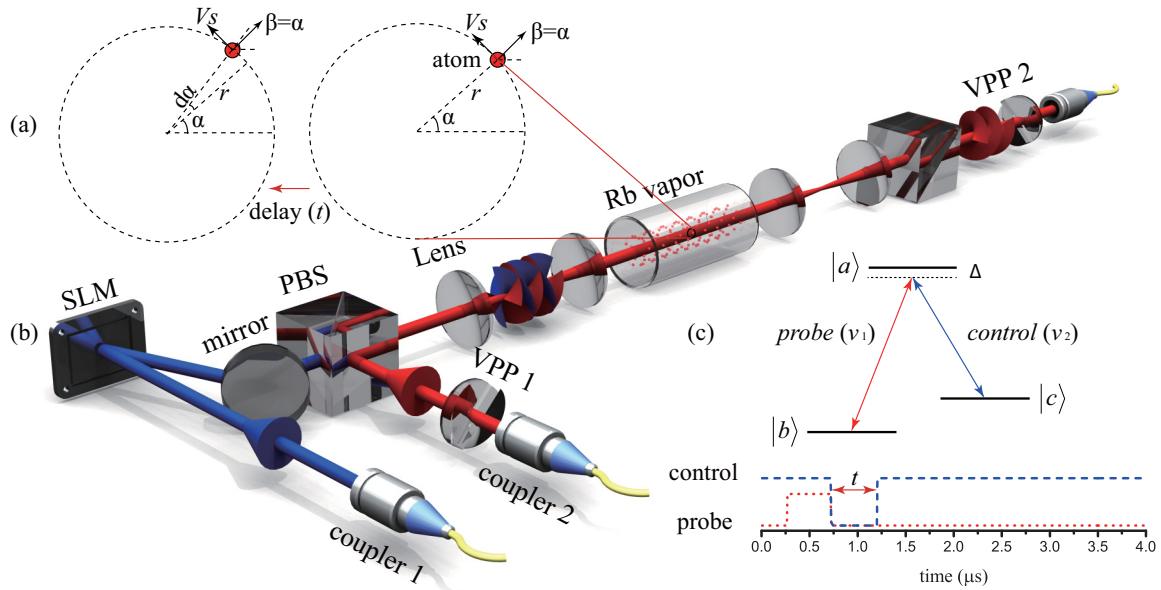


FIG. 1. Experimental setup for optical vortex storing. (a) Illustration of the SW dephasing induced by atomic random motion along the azimuthal direction. (b) The experimental setup. SLM: spatial light modulator; VPP: vortex phase plate; PBS: polarizing beam splitter. (c) The energy level scheme of the  $D_1$  transition of  $^{85}\text{Rb}$  showing the three levels of the  $\Lambda$  system.  $|a\rangle$ ,  $|b\rangle$ , and  $|c\rangle$  correspond to atomic states  $5^2P_{1/2} F = 2$ ,  $5^2S_{1/2} F = 2$ , and  $5^2S_{1/2} F = 3$ , respectively. Time sequence of the experiment is shown at the bottom.

passing through an AOM. A schematic of the experimental setup is shown in Fig. 1(b). The control beam from coupler 1 is diffracted off a computer-generated fork-diffraction pattern on a spatial light modulator (SLM; Holoeye LETO LCoS). The fork dislocation in the pattern introduces a helical phase front  $[\exp(im\alpha)]$  to the first-order diffracted pulse;  $\alpha$  represents an azimuthal angle, thereby imparting an OAM of  $m$ . The probe beam from coupler 2 gets an OAM of  $n$  after passing through vortex phase plate 1 (VPP). The control and the probe are recombined on a polarizing beam splitter (PBS) and copropagate toward a vapor cell. The planes of the SLM and the VPP 1 are imaged onto the center of the vapor cell by using a  $4f$  imaging system, which consists of two lenses with a focal length  $f = 300$  mm. Therefore the control and the probe are shaped as Laguerre-Gaussian (LG) beams with a waist of  $w = 2$  mm (at the center of the vapor cell). We optimize the experiment by adjusting the temperature of the cell and the power of the beam. The power of the control field is 9 mW. A 5-cm-long vapor cell containing  $^{85}\text{Rb}$  is used. The temperature of the cell is stabilized at  $55^\circ\text{C}$ , providing a rubidium vapor density of  $\sim 2.2 \times 10^{11}/\text{cm}^3$ . The cell is placed inside a five-layered magnetic shield. After the beams pass through the vapor cell, another PBS is used to isolate the control beam, and a  $4f$  imaging system is used to isolate the plane of VPP 1 onto VPP 2. VPP 2 with a helical surface opposite to VPP 1 can be used to “flatten” the phase of the probe beam, and then the probe beam is collected into coupler 3. In addition to polarization filtering, we also performed a frequency filtering by using a temperature-controlled Fabry-Perot (FP) etalon. Finally, the probe beam is detected by a photomultiplier tube (PMT; HAMAMATSU H10721-01). The frequency shift between the control and the probe is set to the center of the EIT resonance.

The time sequence of the experiment is shown in Fig. 1(c). At first, we prepare a substantial atomic population into the  $|b\rangle$  state by applying the control beam for a long duration. Then a vortex probe pulse with a duration of 500 ns is sent into the cell. The control beam is turned off to store the probe pulse as an atomic ground-state SW, when the probe pulse is propagating in the vapor cell. The decoherence of the SW occurs during the storage. The control beam is turned on after a certain duration to retrieve the probe pulse, which is finally detected by the PMT. We study the decoherence effect by measuring the write-store-retrieve efficiency [27] (the ratio of energies carried by the retrieved and input signal pulses) for different storage duration.

In the experiment, VPP 1 introduces OAM  $n = 2$  to the probe pulse; we study the effect of dephasing by using a control beam with OAM of  $m = 2, 0$ , and  $-2$ , respectively. The measured lifetime  $\tau$  decreases as the OAM difference between the control and the probe increases, which implies that the decoherence is related to the azimuthal phase gradient of the stored SW.

The experimental result is shown in Fig. 2. We find that the decoherence mechanism of the storage can be explained by the dephasing of the SW induced by atomic random motion. The longitudinal decoherence mechanism has been explored in previous experiments [16,23], but the transverse azimuthal decoherence mechanism has not attracted enough attention yet. As the longitudinal decoherence is related to the wavelength of the SW, the transverse azimuthal decoherence is related to the topological charge of the SW, which is determined by the OAM difference between the control and the probe.

We assume that the Rabi frequencies of the control and the probe are  $\Omega_1$  and  $\Omega_2$ , respectively. The interaction between

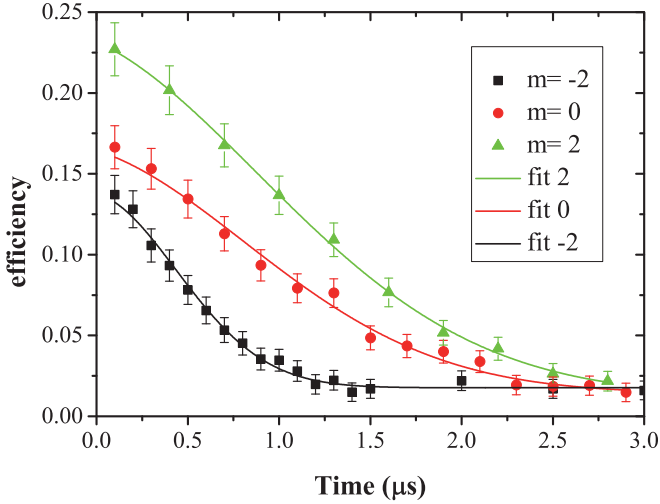


FIG. 2. Lifetime measurement results for control beams with different OAMs and a probe beam with OAM 2. The data are fitted by using  $\eta(t) = C_1 + C_2 e^{-t^2/\tau_D^2} e^{-t/\tau_1}$ . The black curve corresponds to the case of the control beam with OAM  $-2$ , lifetime  $\tau_D = 0.76 \pm 0.03 \mu\text{s}$ ; the red curve corresponds to the control beam with OAM 0, lifetime  $\tau_D = 3.18 \pm 0.75 \mu\text{s}$ ; the green curve represents the case of the control beam with OAM 2, no azimuthal dephasing. All of these curves have a common longitudinal lifetime  $\tau_0 = 1.74 \pm 0.16 \mu\text{s}$  and a lifetime  $\tau_1 = 4.2 \pm 1.5 \mu\text{s}$  due to other decoherence mechanisms. Error bars are calculated from the background standard error of the detector and the 5% error in the memory efficiency.

light and atoms is governed by the Hamiltonian:

$$H_I = -\frac{\hbar}{2}\Omega_1 e^{i\alpha} |a\rangle\langle b| - \frac{\hbar}{2}\Omega_2 e^{-i\phi_2} e^{i\alpha} |a\rangle\langle c| + \text{H.c.} \quad (1)$$

Here  $\exp(i\alpha)$  is the azimuthal phase, which reflects the OAM of the control and the probe. We use collective, slowly varying atomic operators to describe the quantum properties of the atoms:

$$\hat{\sigma}_{\alpha\beta}(z, t) = \frac{1}{N_z} \sum_{j=1}^{N_z} |\alpha_j\rangle\langle\beta_j| e^{-i\omega_{\alpha\beta} t}. \quad (2)$$

Here  $N_z$  is the number of particles contained in the volumes at position  $z$ .

The atomic evolution is governed by a set of Heisenberg-Langevin equations [6]. Under the assumption that the Rabi frequency of the probe is much smaller than that of the control and that the number of photons contained in the input pulse is much less than the number of atoms, the lowest nonvanishing order of  $\hat{\sigma}_{bc}(z, t)$  is

$$\hat{\sigma}_{bc}(z, t) = -g \frac{\Omega_2}{\Omega_1} e^{i(n-m)\alpha}. \quad (3)$$

We can decelerate and stop the input light pulse by adiabatically turning off the control beam. In this process, the azimuthal phase difference between the probe and the control is mapped onto collective states of the matter, in which they are stored.

The decoherence induced by atomic random motion can be divided into three kinds, as atoms move in a three-dimensional

space. The first one is caused by random movement of atoms along the wave-vector direction of the SW, which results in a phase fluctuation [23]. The second one is atomic movement along the transverse radial direction; atoms from all directions carrying a phase destructively interfere at the dark center which is a phase singularity of the SW [20,24]. The final one is atomic movement along the transverse azimuthal direction, which results in a phase front fluctuation. It can be understood as follows. We take the case of  $l = n - m = 1$  for intuitively understanding. As shown in Fig. 1(a), an optical pulse with OAM is stored in the atomic ensemble as the SW with azimuthal phase  $\beta$  equal to the azimuthal angle  $\alpha$ , and it will be retrieved after a delay time  $t$ . During this interval, each atom with phase  $\beta$  moves from one azimuthal point to another randomly. The internal states of the atoms are conserved. However, the azimuthal motion of the atoms leads to a perturbation on the phase front of the SW. Consequently, the projection of the perturbed SW on the original state gradually decreases as the delay time  $t$  increases. Therefore, the atomic azimuthal motion leads to a random phase front fluctuation to the SW and thus it causes decoherence. The time scale of the dephasing can be estimated by calculating the average time by which the atoms cross  $1/2\pi$  of the azimuthal period of the SW. Atoms at different radial positions need to cross a different distance to move the same azimuthal angle; the lifetime  $\tau_D(r)$  is changing with radial position  $r$ :  $\tau_D(r) \sim (r/lv_S)$ , with  $v_S = \sqrt{k_B T/m}$  the one-dimensional average speed, where  $k_B$  is the Boltzman constant,  $T$  the average temperature of the cell, and  $2\pi/l$  the azimuthal period angle of the SW. The intensity of the spin wave is in Gaussian distribution, because the planes of the SLM and the VPP 1 are imaged onto the center of the vapor cell by the  $4f$  system. The Gaussian weighted average lifetime is

$$\tau_D \sim \int \tau_D(r) \frac{4r}{W_0^2} \exp\left[-\frac{2r^2}{W_0^2}\right] dr = \frac{\sqrt{2\pi} W_0}{4lv_S}. \quad (4)$$

Here  $W_0$  is the beam waist. A more detailed calculation yields the retrieval efficiency,  $\gamma(t) \sim e^{-t^2/\tau_D^2}$ , with a lifetime of  $\tau_D = \frac{\sqrt{2\pi} W_0}{4lv_S}$ . Assume that the  $j$ th atom is excited to  $|\psi_{j0}\rangle = e^{i\alpha_j(0)} |c\rangle$  at time  $t = 0$ , and moves to azimuthal position  $\alpha_j(t) = \alpha_j(0) + (v_j/r)t$  after a storage time of  $t$ . The state freely evolves to  $|\psi_{jt}\rangle = e^{i\alpha_j(t)} |c\rangle$ ; the retrieval efficiency of the  $j$ th atom is proportional to the overlap between the original state and the perturbed one,

$$\gamma_j(t) \sim |\langle\psi_{j0}|\psi_{jt}\rangle|^2 = |e^{i(v_j/r)t}|^2 = \left| \int f(v) e^{i(v/r)t} dv \right|^2, \quad (5)$$

with  $f(v) \sim e^{-mv^2/2k_B T}$  being a Boltzmann distribution of the velocity at temperature  $T$ . Integrating over all possible velocities, we obtain  $\gamma_j(t) \sim e^{-t^2/\tau_D^2}$ , with the lifetime  $\tau_D(r) = (r/lv_S)$ . This atom contributes  $1/n$  to the overall retrieval efficiency; the total retrieval efficiency is  $\gamma(t) = \frac{1}{n} \sum_j \gamma_j(t)$ , with  $n$  being the number of total excited atoms. The Gaussian weighted average lifetime is  $\tau_D = \frac{\sqrt{2\pi} W_0}{4lv_S}$ . In our case, the OAM difference between the control and the probe determines the topological charge  $l = n - m$ , which is related to the lifetime of the SW. In order to confirm that the decoherence

is mainly caused by atomic azimuthal motion, we increase the topological charge of the SW by decreasing the OAM of the control (see Fig. 2). According to the above model, the dephasing will be enhanced and the lifetime will be shortened. In our experiment, we use the control with OAM 2, 0, and  $-2$  to measure the lifetime of the quantum memory for each case; the experimental results, shown in Fig. 2, are fitted by a total decay function:

$$\eta(t) = C_1 + C_2 e^{-t^2/\tau_D^2} e^{-t^2/\tau_0^2} e^{-t/\tau_1}. \quad (6)$$

Here  $C_1 \approx 0.015$  is the background noise level, which depends on the dark current of the PMT.  $C_2$  is the retrieval efficiency at  $t = 0$ :  $C_2 = 0.22 \pm 0.01$  for control beam  $m = 2$ ,  $C_2 = 0.150 \pm 0.005$  for  $m = 0$ , and  $C_2 = 0.120 \pm 0.003$  for  $m = -2$ .  $C_2$  depends on the interaction between the probe and the control beam which will be discussed later. The decay includes three parts: The first one,  $e^{-t^2/\tau_D^2}$ , has been explained above; the second one  $e^{-t^2/\tau_0^2}$  is caused by atomic longitudinal random motion [23]; and the third one,  $e^{-t/\tau_1}$ , is caused by other decoherence processes [4]. SWs with different topological charges have a common longitudinal lifetime  $\tau_0$ , because the wavelength and other properties of the SWs are the same. We extract  $\tau_0 = 1.74 \pm 0.16 \mu\text{s}$  and  $\tau_1 = 4.2 \pm 1.5 \mu\text{s}$  from the fit of SW with 0 OAM at first. Then we obtain lifetimes of  $\tau_D = 3.18 \pm 0.75 \mu\text{s}$  for  $l = 2$  and  $\tau_D = 0.76 \pm 0.03 \mu\text{s}$  for  $l = 4$ . As expected, the lifetime decreases as the topological charge of the SW increases. Our results clearly show that the dephasing of the SW is sensitive to the OAM difference between the probe and the control, and that a SW with high topological charge is extremely sensitive to the atomic random motion. All the adjusted  $R$ -squared (the result of a chi-square test which reflects the suitability of the theoretical model) of the fitted curves are greater than 98%. This indicates that the above model is in good agreement with the experimental results.

To further confirm the relationship between the retrieval efficiency and the topological charge of the SW, we measure the retrieval efficiencies after storage of 0.1, 0.5, and 1.5  $\mu\text{s}$  for SWs with different topological charges (Fig. 3). We found that the dependencies follow Gaussian curves, the centers of which correspond to SW with zero topological charge; the full width at half maximum (FWHM) decreases as the storage time increases.

This relationship can be understood as follows. We take the azimuthal lifetime  $\tau_D = \frac{\sqrt{2\pi}W_0}{4lv_s}$  into the total decay function, Eq. (6), and assume that all parameters except  $l$  are constant; then we get  $\eta(l) = C_1 + C_2 e^{-Bl^2}$ , which is clearly a Gaussian function. Moreover, the decrease of the FWHM indicates that SW with higher topological charge has a faster decoherence rate.

The retrieval efficiency at  $t = 100 \text{ ns}$  is close to that at  $t = 0 \text{ ns}$ . The curve for  $t = 100 \text{ ns}$  follows the Gaussian curve which indicates that the retrieval efficiency at  $t = 0 \text{ ns}$  is different for different  $l$ . The greater the difference between the control and the probe beam, the weaker the interaction, but more detailed and quantitative investigation of the functional form and dependence of this relationship should be performed in the future.

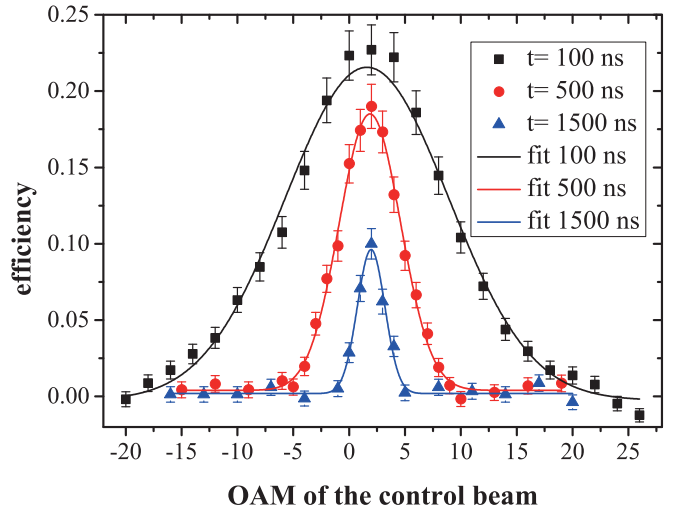


FIG. 3. Retrieval efficiency curves along with the change of the OAM  $m$  of the control beam. The data are fitted by using  $\eta(m) = C_1 + C_2 \exp[-\frac{1}{2}(\frac{m-A}{w})^2]$ . The black curve is for  $t = 100 \text{ ns}$ ,  $w = 7.3 \pm 0.2$ ; the red curve is for  $t = 500 \text{ ns}$ ,  $w = 2.74 \pm 0.07$ ; the blue curve is for  $t = 1500 \text{ ns}$ ,  $w = 1.23 \pm 0.07$ . The adjusted  $R$ -squared is greater than 0.96.

We further verify that this relationship is valid for a probe beam with different OAM of 2 and 20 (Fig. 4). The data are fitted by using  $\eta(m) = C_1 + C_2 \exp[-\frac{1}{2}(\frac{m-A}{w})^2]$ ;  $C_1$  is the background noise level:  $C_1 \approx 0.03$ .  $C_2$  is the retrieval efficiency of SW with 0 OAM:  $C_2 = 0.181 \pm 0.005$  for  $n = 2$  and  $C_2 = 0.12 \pm 0.005$  for  $n = 20$ . The decrease of  $C_2$  is because the interaction between the probe and control beam decreases as  $n$  increases.  $A$  is the center of the Gaussian curves:  $A = 1.86 \pm 0.07$  for  $n = 2$  and  $A = 19.7 \pm 0.1$  for  $n = 20$ . The fitting value  $A \approx n$  is in agreement with the theory.

Finally, we prove that the lifetime is also related to the size of the SW, which is determined by the waist of the probe and the control beams. We change one of the two lenses in the 4f

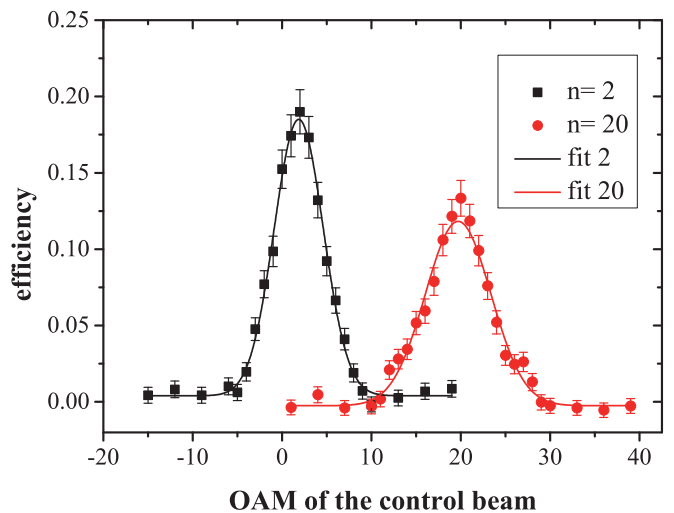


FIG. 4. Retrieval efficiency curves along with the change of the OAM  $m$  of the control beam. The black and red curves corresponding to the probe with OAM  $n = 2$  and 20, respectively. The adjusted  $R$ -squared is greater than 0.97.

system to zoom in and out on the waist of the beams. Since a SW with a bigger size is mainly stored by atoms located further from the beam center, the atoms need to move a greater distance to induce the same phase shift. So an OAM SW with a bigger size is more robust to atomic motion; therefore its lifetime is longer. As expected, the lifetime  $\tau_D$  is  $0.43 \pm 0.01 \mu\text{s}$  for a 1.2-mm waist,  $0.63 \pm 0.05 \mu\text{s}$  for a 2-mm waist, and  $0.89 \pm 0.04 \mu\text{s}$  for a 3.34-mm waist (see Fig. 5). We experimentally observe an increase in the lifetime for an OAM SW as the beam waist increases, but more detailed and quantitative investigation of the functional form and dependence of this relationship should be performed in the future (in order to verify the linear relationship predicted in our theoretical model).

In our experiment, we have divided the decoherence mechanisms induced by atomic random motion into three kinds, and we thoroughly investigated the transverse azimuthal dephasing of the stored SW by varying its topological charge. A theoretical explanation in accordance with experimental results is given. Our experiment reveals the transverse azimuthal dephasing mechanism of the SW with OAM, so the storage of light with higher OAM has a faster decoherence rate. In order to increase the storage time of light with high OAM, we can introduce OAM to the control beam to suppress the transverse azimuthal dephasing. According to the theory, the decoherence of SW with topological charge is induced by the transverse azimuthal motion of atoms, so experimental systems which can eliminate the transverse motion of atoms are suitable for storing high-dimensional light, such as an optical lattice, a Rb-filled photonic crystal fiber, etc.

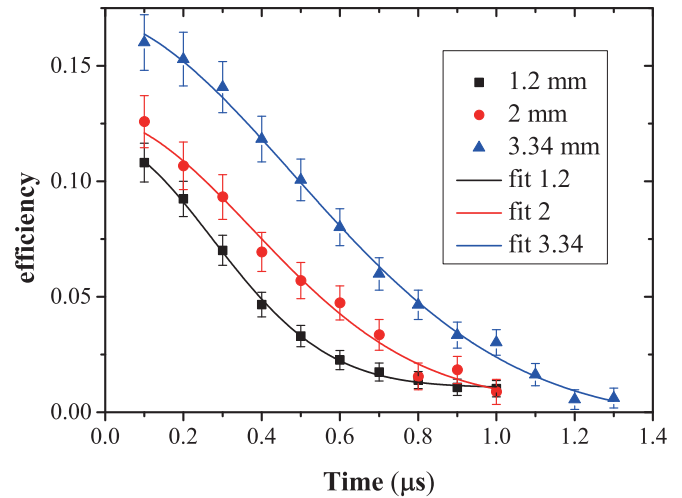


FIG. 5. Lifetime measurement results for SWs with different waists. The black curve is for a 1.2-mm waist, lifetime  $\tau_D = 0.43 \pm 0.01 \mu\text{s}$ ; the red curve is for a 2-mm waist, lifetime  $\tau_D = 0.63 \pm 0.05 \mu\text{s}$ ; the blue curve is for a 3.34-mm waist, lifetime  $\tau_D = 0.89 \pm 0.04 \mu\text{s}$ . The adjusted  $R$ -squared is greater than 0.98.

This work was supported by the National Natural Science Foundation of China (Grants No. 11604322, No. 61605194, No. 61275115, No. 61435011, and No. 61525504).

[1] H. J. Briegel, W. Dür, J. I. Cirac, and P. Zoller, *Phys. Rev. Lett.* **81**, 5932 (1998).  
 [2] E. Knill, R. Laflamme, and G. J. Milburn, *Nature* **409**, 46 (2001).  
 [3] O. Firstenberg, M. Shuker, A. Ron, and N. Davidson, *Rev. Mod. Phys.* **85**, 941 (2013).  
 [4] C. Mewes and M. Fleischhauer, *Phys. Rev. A* **72**, 022327 (2005).  
 [5] M. D. Eisaman, A. André, F. Massou, M. Fleischhauer, A. Zibrov, and M. Lukin, *Nature* **438**, 837 (2005).  
 [6] M. Fleischhauer and M. D. Lukin, *Phys. Rev. Lett.* **84**, 5094 (2000).  
 [7] D. F. Phillips, A. Fleischhauer, A. Mair, R. L. Walsworth, and M. D. Lukin, *Phys. Rev. Lett.* **86**, 783 (2001).  
 [8] R. M. Camacho, C. J. Broadbent, I. Ali-Khan, and J. C. Howell, *Phys. Rev. Lett.* **98**, 043902 (2007).  
 [9] M. Shuker, O. Firstenberg, R. Pugatch, A. Ron, and N. Davidson, *Phys. Rev. Lett.* **100**, 223601 (2008).  
 [10] M. V. Balabas, T. Karaulanov, M. P. Ledbetter, and D. Budker, *Phys. Rev. Lett.* **105**, 070801 (2010).  
 [11] M. A. Bouchiat and J. Brossel, *Phys. Rev.* **147**, 41 (1966).  
 [12] O. Kocharovskaya, Y. Rostovtsev, and M. O. Scully, *Phys. Rev. Lett.* **86**, 628 (2001).  
 [13] Y. Xiao, M. Klein, M. Hohensee, L. Jiang, D. F. Phillips, M. D. Lukin, and R. L. Walsworth, *Phys. Rev. Lett.* **101**, 043601 (2008).  
 [14] O. Firstenberg, M. Shuker, N. Davidson, and A. Ron, *Phys. Rev. Lett.* **102**, 043601 (2009).  
 [15] G. Hétet, M. Hosseini, B. M. Sparkes, D. Oblak, P. K. Lam, and B. C. Buchler, *Opt. Lett.* **33**, 2323 (2008).  
 [16] J. Rui, Y. Jiang, S. J. Yang, B. Zhao, X.-H. Bao, and J.-W. Pan, *Phys. Rev. Lett.* **115**, 133002 (2015).  
 [17] P. K. Vudyasetu, R. M. Camacho, and J. C. Howell, *Phys. Rev. Lett.* **100**, 123903 (2008).  
 [18] O. Firstenberg, P. London, D. Yankelev, R. Pugatch, M. Shuker, and N. Davidson, *Phys. Rev. Lett.* **105**, 183602 (2010).  
 [19] D. Yankelev, O. Firstenberg, M. Shuker, and N. Davidson, *Opt. Lett.* **38**, 1203 (2013).  
 [20] R. Pugatch, M. Shuker, O. Firstenberg, A. Ron, and N. Davidson, *Phys. Rev. Lett.* **98**, 203601 (2007).  
 [21] D. S. Ding, Z. Y. Zhou, B. S. Shi, and G. C. Guo, *Nat. Commun.* **4**, 2527 (2013).  
 [22] D. S. Ding, W. Zhang, Z. Y. Zhou, S. Shi, G. Y. Xiang, X. S. Wang, Y. K. Jiang, B. S. Shi, and G. C. Guo, *Phys. Rev. Lett.* **114**, 050502 (2015).  
 [23] B. Zhao, Y. A. Chen, X. H. Bao, T. Strassel, C. S. Chu, X. M. Jin, J. Schmiedmayer, Z. S. Yuan, S. Chen, and J. W. Pan, *Nat. Phys.* **5**, 95 (2009).  
 [24] T. Wang, L. Zhao, L. Jiang, and S. F. Yelin, *Phys. Rev. A* **77**, 043815 (2008).  
 [25] M. Fleischhauer, A. Imamoglu, and J. P. Marangos, *Rev. Mod. Phys.* **77**, 633 (2005).  
 [26] R. A. de Oliveira, L. Pruvost, P. S. Barbosa, W. S. Martins, S. Barreiro, D. Felinto, D. Bloch, and J. W. R. Tabosa, *Appl. Phys. B* **117**, 1123 (2014).  
 [27] I. Novikova, A. V. Gorshkov, and D. F. Phillips, A. S. Sørensen, M. D. Lukin, and R. L. Walsworth, *Phys. Rev. Lett.* **98**, 243602 (2007).